Acta Crystallographica Section B
Structural Science
ISSN 0108-7681

Diffuse scattering and ordering in the short-range modulated paraelectric phase of sodium nitrite, $NaNO_2$

K. Łukaszewicz,* A. Pietraszko and M. Kucharska

Institute of Low Temperature and Structure Research, Polish Academy of Sciences, Okólna 2, 50-950 Wrocław, Poland

Correspondence e-mail: k.lukaszewicz@int.pan.wroc.pl

Received 9 November 2004
Accepted 13 July 2005

The incommensurately modulated antiferroelectric phase of sodium nitrite, $NaNO_2$, transforms at T_N = 437.7 K to the short-range modulated paraelectric phase. The apparently discontinuous phase transition is accompanied by characteristic changes in the diffraction pattern. Contrary to the well known modulated structures with sharp satellite reflections, the diffraction pattern of a short-range modulated structure contains diffuse satellite reflections. The short-range modulated crystal structure of the paraelectric phase of sodium nitrite has been analysed by the Reverse Monte Carlo (RMC) simulation of X-ray diffuse scattering. The crystal structure of sodium nitrite may be regarded as consisting of $[Na^+NO_2^-]_\infty$ rows running along the polar *b* axis. One can expect long fragments of rows with uniform polarity The assumption that single $[Na^+NO_2^-]_\infty$ rows are polar with uniform polarity proved to be a convenient approximation which is in good agreement with the observed diffraction pattern. The distribution of (+)- and (−)-$[Na^+NO_2^-]_\infty$ polar rows crossing the (010) plane of short-range modulated $NaNO_2$ revealed by RMC shows nanodomains consisting of distorted fragments of a sinusoidally modulated crystal structure. The size of the nanodomains and the degree of order in paraelectric $NaNO_2$ decreases with temperature.

1. Introduction and summary of previous work

Crystals of $NaNO_2$ are orthorhombic with the space group *Im*2*m* in the ferroelectric phase and *Immm* in the paraelectric phase. The crystal structure of sodium nitrite was determined at room temperature by Ziegler (1931). The ferroelectric properties of $NaNO_2$ discovered by Sawada *et al.* (1958) stimulated a series of papers on the crystal structure determination of $NaNO_2$ over a broad range of temperature, *e.g.* Kay *et al.* (1975, 1992) and others. Recently the crystal structure of ferroelectric $NaNO_2$ at 30 K has been published by Gohda *et al.* (2000), and that of paraelectric $NaNO_2$ at 458 K by Ichikawa *et al.* (2002).

Tanisaki (1961) reported an antiferroelectric incommensurately modulated phase of $NaNO_2$ extending above the Curie point T_C = 436.2 K up to T_N = 437.7 K. Hoshino & Motegi (1967) described the crystal structure of antiferroelectric $NaNO_2$ with the sinusoidal modulation of electric dipole moments while the modulation length decreases with temperature from 10.3*a* to 8.4*a*. The crystal structure of the antiferroelectric phase with a sinusoidal occupancy modulation of (+)- and (−)-oriented $Na^+NO_2^-$ dipoles has been determined by Kucharczyk *et al.* (1978) with an additional sinusoidal displacement of dipoles along the polar axis. Boehm (1978) solved the crystal structure of $NaNO_2$ just above the

© 2005 International Union of Crystallography
Printed in Great Britain – all rights reserved

Curie point as an eightfold superstructure with a sinusoidal displacement of Na atoms.

Sodium nitrite, $NaNO_2$, transforms at $T_N = 437.7$ K from the incommensurately modulated antiferroelectric phase to the short-range modulated paraelectric phase. Contrary to the well known modulated structures with sharp satellite reflections, the diffraction pattern of a short-range modulated structure contains diffuse satellite reflections. The phase transition is accompanied by characteristic changes in the diffraction. Yamada *et al.* (1963) reported characteristic temperature changes of the 042 reflection. At $T_N = 437.7$ K the Bragg reflection 042 with no satellites disappears and is replaced by the strong diffuse satellite reflections $(0 \pm \sigma)42$, decreasing slowly with temperature. The behavior of the 150 Bragg reflection and its satellites was reported by Hoshino & Motegi (1967). Sharp satellite $(1 \pm \sigma)50$ reflections disappear on approaching T_N and are replaced by diffuse reflections. Canut & Hosemann (1964) investigated the diffuse scattering of $NaNO_2$ in the paraelectric phase 20 K above the Curie point and found microdomains of a characteristic shape which they called 'cigarillos'.

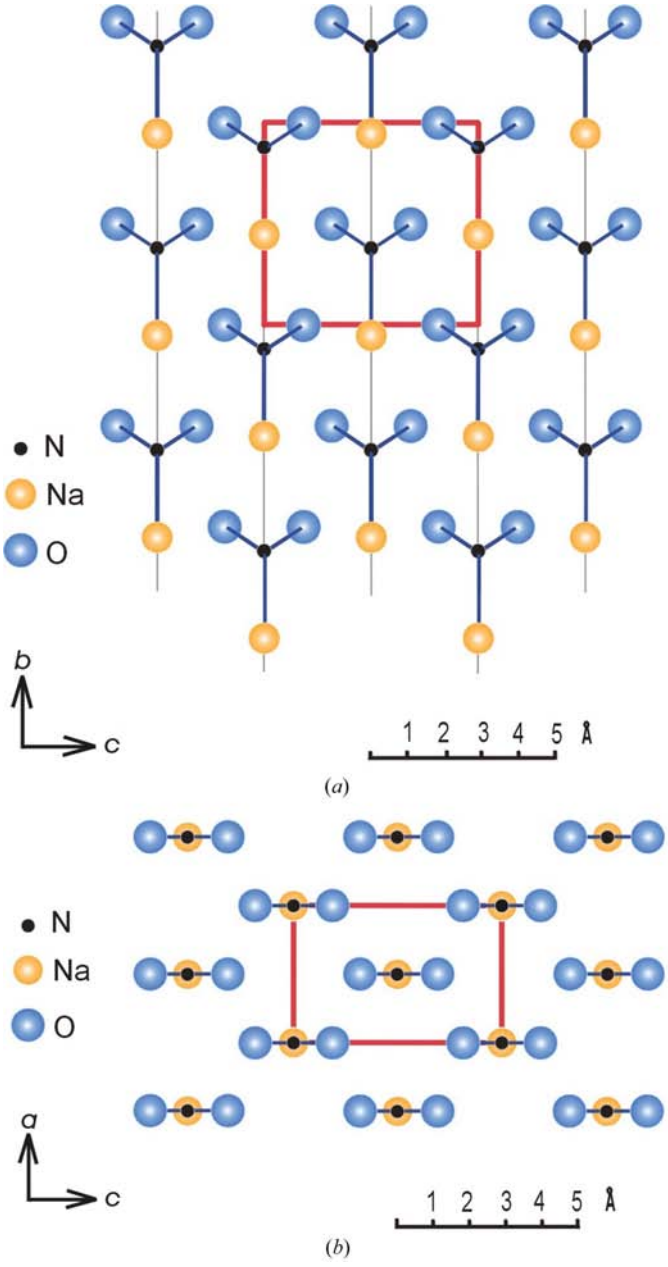

Figure 1
The crystal structure of ferroelectric $NaNO_2$ with $[Na^+NO_2^-]_\infty$ rows viewed along (*a*) [100] and (*b*) [010].

We have undertaken the study of the temperature dependence of the diffuse scattering and the short-range modulation of paraelectric $NaNO_2$. It was therefore necessary to design a convenient and realistic model for the short-range modulated crystal structure of $NaNO_2$. In the ferroelectric phase the crystal structure of sodium nitrite may be regarded as consisting of infinite rows of $[Na^+NO_2^-]_\infty$ running along the polar [010] axis. The crystal structure of ferroelectric $NaNO_2$ with $[Na^+NO_2^-]_\infty$ rows viewed along [100] is shown in Fig. 1(*a*) and along [010] in Fig. 1(*b*). Owing to the body centering of the lattice cell, every second chain is shifted by $\frac{1}{2}a + \frac{1}{2}b + \frac{1}{2}c$. On heating, the polarity of some fragments of the $[Na^+NO_2^-]_\infty$ rows may become reversed. The opposite polarity of neighboring fragments in a single row is energetically unfavorable so one can therefore expect long sections of rows with uniform polarity. It was hence convenient to assume as a reasonably good approximation that single infinite $[Na^+NO_2^-]_\infty$ rows were of uniform polarity.

This assumption considerably simplified calculations, thus allowing us to reduce the problem to two dimensions. Rather than discussing a three-dimensional distribution of polar fragments of $[Na^+NO_2^-]_\infty$ rows, we studied a distribution of (+) or (−) infinite polar rows $[Na^+NO_2^-]_\infty$ crossing the (010) plane. Good agreement between the observed and calculated diffraction patterns based on the assumption of infinite $[Na^+NO_2^-]_\infty$ rows of uniform polarity has proved this assumption to be sufficient.

Above the Curie point in the antiferroelectric and paraelectric phases the crystal structure of $NaNO_2$ consists of equal numbers of (+)- and (−)-$[Na^+NO_2^-]_\infty$ rows. The physical properties and diffraction pattern of $NaNO_2$ at each temperature point depend on the distribution of (+) and (−) rows in the crystal structure.[1]

2. Experimental

Crystals for this study were from the same origin as those used by Kucharczyk *et al.* (1978). Recording the diffuse scattering required a larger than usual crystal specimen of the dimensions 0.22 × 0.28 × 0.33 mm. Diffraction data were obtained with a KUMA Diffraction KM4CCD four-circle diffractometer equipped with a CCD detector. Graphite-monochromated Mo $K\alpha$ X-rays, $\lambda = 0.71073$ Å, were generated at 50 kV and 23 mA. Three-dimensional sets of X-ray diffraction data were collected in the range 3–55° 2θ. The data were

[1] Supplementary data for this paper are available from the IUCr electronic archives (Reference: CK5007). Services for accessing these data are described at the back of the journal.

collected with $\Delta\omega = 0.25^\circ$. At all temperatures the recording time of a single frame was 45 s.

The crystal structure of paraelectric $NaNO_2$ at 458 K has been published previously (Kay *et al.*, 1992; Komatsu *et al.*, 1988; Ichikawa *et al.*, 2002). The thermal expansion of paraelectric $NaNO_2$ is anisotropic. Lattice parameters *a* and *b* increase, while *c* decreases with temperature (Kucharczyk *et al.*, 1976). It was therefore important to determine the lattice and atomic parameters of short-range modulated paraelectric $NaNO_2$ at 438, 442, 460 and 480 K based on data collected while studying diffuse scattering. The data collected when recording diffuse scattering were not very suitable for crystal structure determination, but the accuracy of the lattice and atomic parameters presented in Table 1 was nevertheless sufficient for RMC simulation.

3. Data reduction and processing

Layers of the reciprocal lattice were reconstructed using the *CrysAlis* program, Version 169. There are a few options for reconstructing a definite layer. The layer may be a one-pixel cross-section of the reciprocal lattice corrected for *Lp* and presented in *CrysAlis* format with 512 × 512 pixels. In the case of diffuse scattering it is useful to display the average of several parallel cross-sections in a thin slice of the reciprocal lattice. In our study we reconstructed the *h*4*l* layer of the

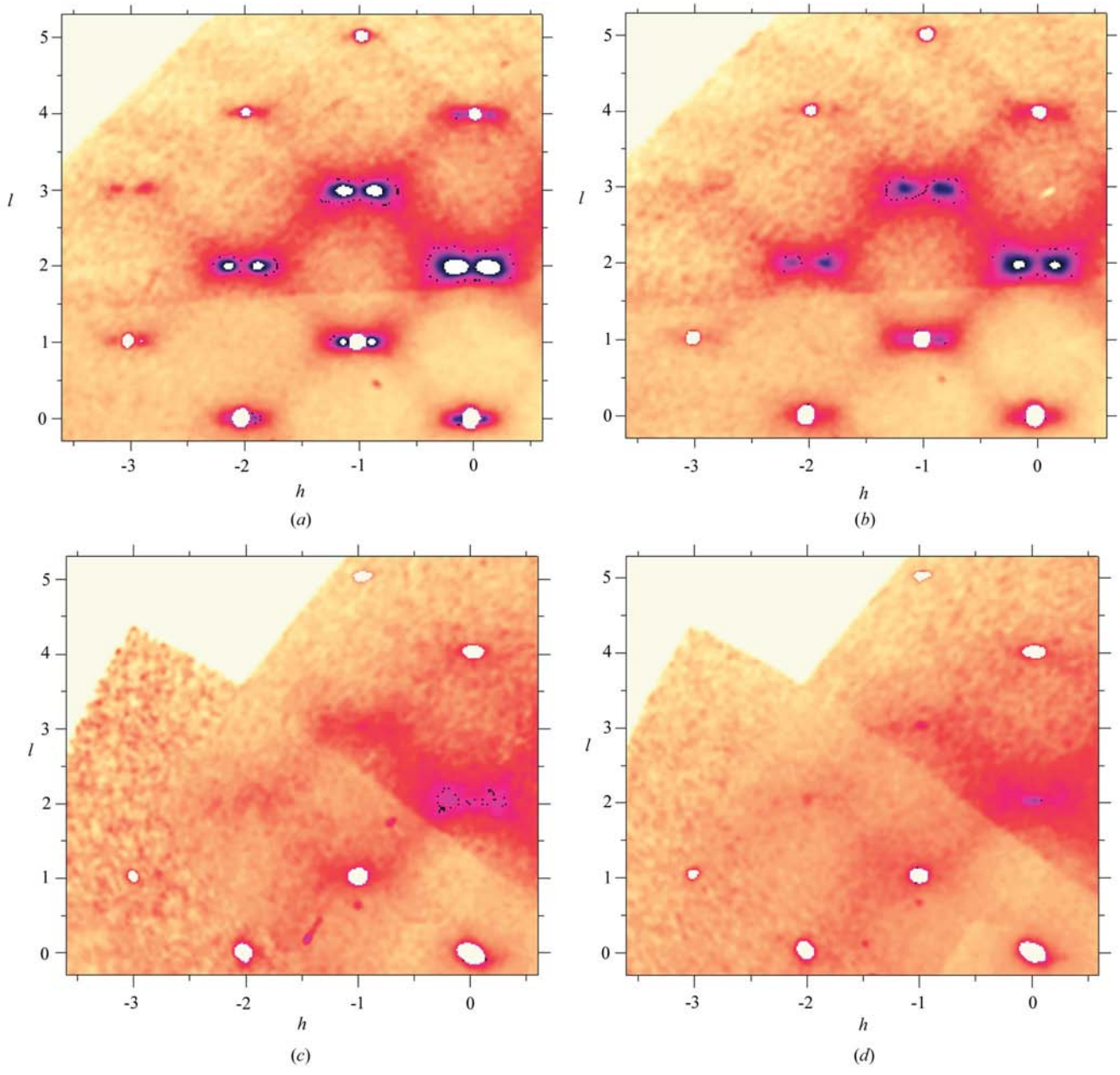

Figure 2
A portion of the *h*4*l* layer of $NaNO_2$ containing diffuse satellite reflections reconstructed by the program *CrysAlis*: (*a*) at 438 K, (*b*) at 442 K, (*c*) at 460 K and (*d*) at 480 K.

diffraction pattern by averaging nine parallel cross-sections of the reciprocal lattice in a thin slice with k = 3.96–4.04.

The resolution of the reciprocal lattice layer reconstructed using the *CrysAlis* program depends on the correct selection of the r parameter. In the reciprocal lattice layer 1 Å^{-1} corresponds to 256 pixels. In the hKl (K = constant) layer the distance N[100] between the pairs of reflections hKl and $(h+1)Kl$ is expressed by the number of pixels N[100] = 256r pixels Å^{-1} a^* Å^{-1} and $N(001)$ = 256r pixels Å^{-1} c^* Å^{-1}. For the $h4l$ layer reconstructed with r = 1, $a^* \simeq 0.273$ Å^{-1} and $c^* \simeq 0.186$ Å^{-1}, N[100] $\simeq$ 70 and $N(001) \simeq 48$.

4. Reverse Monte Carlo (RMC) simulation

The Reverse Monte Carlo (RMC) simulation of the whole recorded diffraction pattern of $NaNO_2$ would require computational power that was not actually available. We decided, therefore, to apply a simplified model of the crystal structure of $NaNO_2$ consisting of infinite $[Na^+NO_2^-]_\infty$ rows of uniform polarity. The distribution of (+) or (−) polar rows of $[Na^+NO_2^-]_\infty$ passing through 0,0,0 and $\frac{1}{2}$,0,$\frac{1}{2}$ sites of the lattice cells in the (010) plane was obtained by the RMC simulation of a portion of the $h4l$ layer containing characteristic diffuse satellite reflections $(0 \pm \sigma)42$, $(2 \pm \sigma)42$, $(1 \pm \sigma)43$ and $(3 \pm \sigma)43$ with $\sigma \simeq 1/8$. Additionally, diffuse satellite reflec-

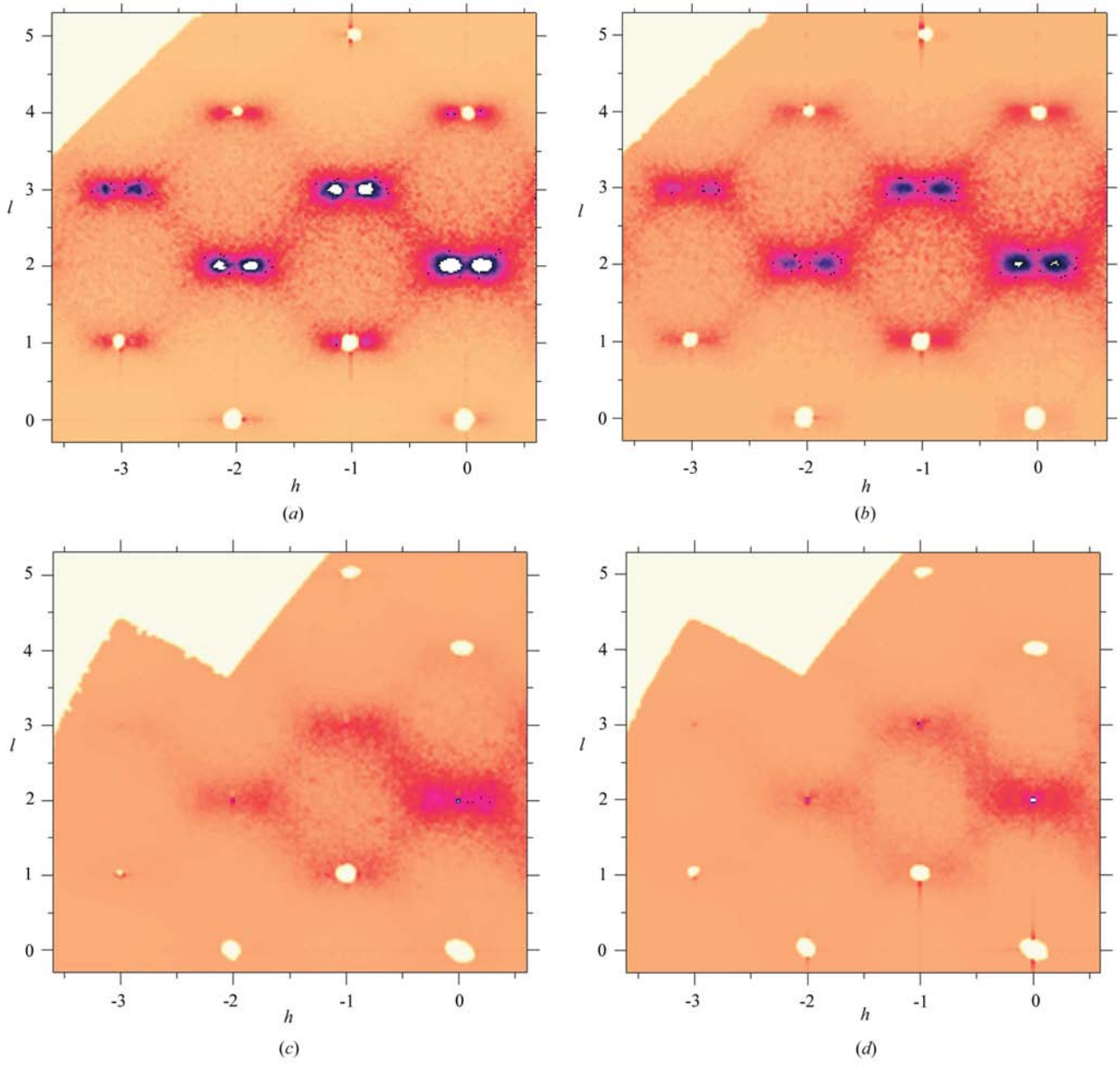

Figure 3
A portion of the $h4l$ layer containing diffuse satellite reflections recorded: (*a*) at 438 K, (*b*) at 442 K, (*c*) at 460 K, and (*d*) at 480 K, simulated by RMC.

Table 1
Lattice and atomic parameters of the short- and medium-range modulated paraelectric phase of $NaNO_2$ employed in the RMC simulation.

T (K)	438	442	460	480
a (Å)	3.653 (4)	3.661 (3)	3.685 (4)	3.706 (4)
b (Å)	5.656 (2)	5.667 (3)	5.700 (5)	5.714 (4)
c (Å)	5.385 (4)	5.372 (4)	5.351 (3)	5.335 (3)
y_{Na}	0.538 (1)	0.540 (1)	0.536 (2)	0.535 (2)
y_N	0.072 (1)	0.062 (1)	0.074 (1)	0.074 (1)
y_O	−0.043 (2)	−0.048 (14)	−0.043 (1)	−0.046 (2)
z_O	0.193 (1)	0.196 (2)	0.193 (1)	0.193 (1)
$U_{eq\ Na}$	0.049 (3)	0.035 (3)	0.057 (3)	0.059 (3)
$U_{eq\ N}$	0.052 (3)	0.043 (2)	0.060 (2)	0.066 (2)
$U_{eq\ O}$	0.062 (4)	0.09 (2)	0.067 (3)	0.073 (3)

tions $(0 \pm \sigma)22$ from the *h*2*l* layer were also included. In the RMC procedure we used the program *DISCUS*3.4 (Neder & Proffen, 1997).

The layers of the reciprocal lattice were reconstructed with $r = 1$. Portions of selected reconstructed layers were transferred to the format required by *DISCUS* using a program written by Krawczyk (2002). Strong Bragg reflections were removed because they would dominate the RMC procedure. Satisfactory results of the RMC simulation were obtained with 70×48 simulated lattice cells in the (010) plane corresponding to the resolution of the reconstructed layer. Portions of the *h*4*l* layers of the short-range modulated paraelectric phase of $NaNO_2$ recorded at 438, 442, 460 and 480 K are presented in Figs. 2 (*a*)–(*d*).

The portions of the *h*4*l* layers were RMC simulated by changing the distribution of (+)- and (−)-$[Na^+NO_2^-]_\infty$ chains passing through 0,0,0 and $\frac{1}{2},0,\frac{1}{2}$ sites of a set of 70×48 unit cells in the (010) plane. The simulated layers are presented in Figs. 3(*a*)–(*d*). It is convenient to show the agreement between measured and simulated data by comparing the cross sections through the measured and simulated layers. The cross sections of measured and simulated *h*4*l* layers at $l = 2$ are presented in Figs. 4(*a*)–(*d*). Measured curves are blue and simulated red.

The diffraction pattern of $NaNO_2$ in the short-range modulated paraelectric phase is complicated and rich in

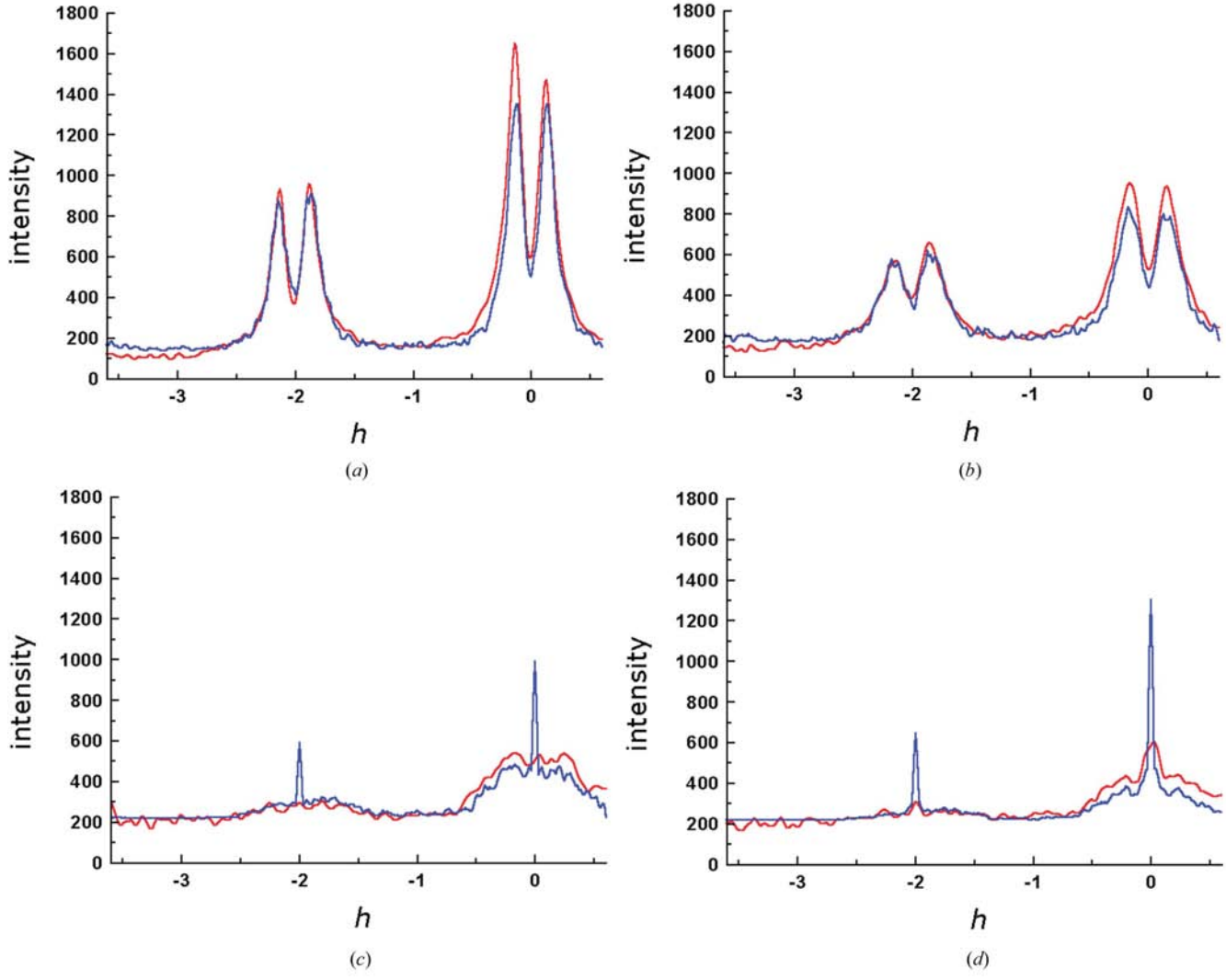

Figure 4
Cross section through the *h*4*l* layer at $l = 2$: (*a*) at 438 K, (*b*) at 442 K, (*c*) at 460 K and (*d*) at 480 K. Measured: red; simulated: blue.

characteristic details. For technical reasons we had to limit the RMC simulation to a small part of a three-dimensional reciprocal lattice and to apply a simplified model of the crystal structure of $NaNO_2$ consisting of infinite (+)- and (−)-$[Na^+NO_2^-]_\infty$ rows.

The refinement was limited to the *h*4*l* layer rich in characteristic details. Other layers are less detailed and much less information can be obtained from them. The RMC refinement based on the *h*4*l* layer is therefore most reliable. In order to confirm the validity of our assumptions and the reliability of the results obtained, we compared the reconstructed *hk*2 and 0.5*kl* layers recorded at 438 K with the same layers calculated by the Fourier transform *DISCUS* program (Neder & Proffen, 1997) based on the disordered crystal structure of $NaNO_2$ at

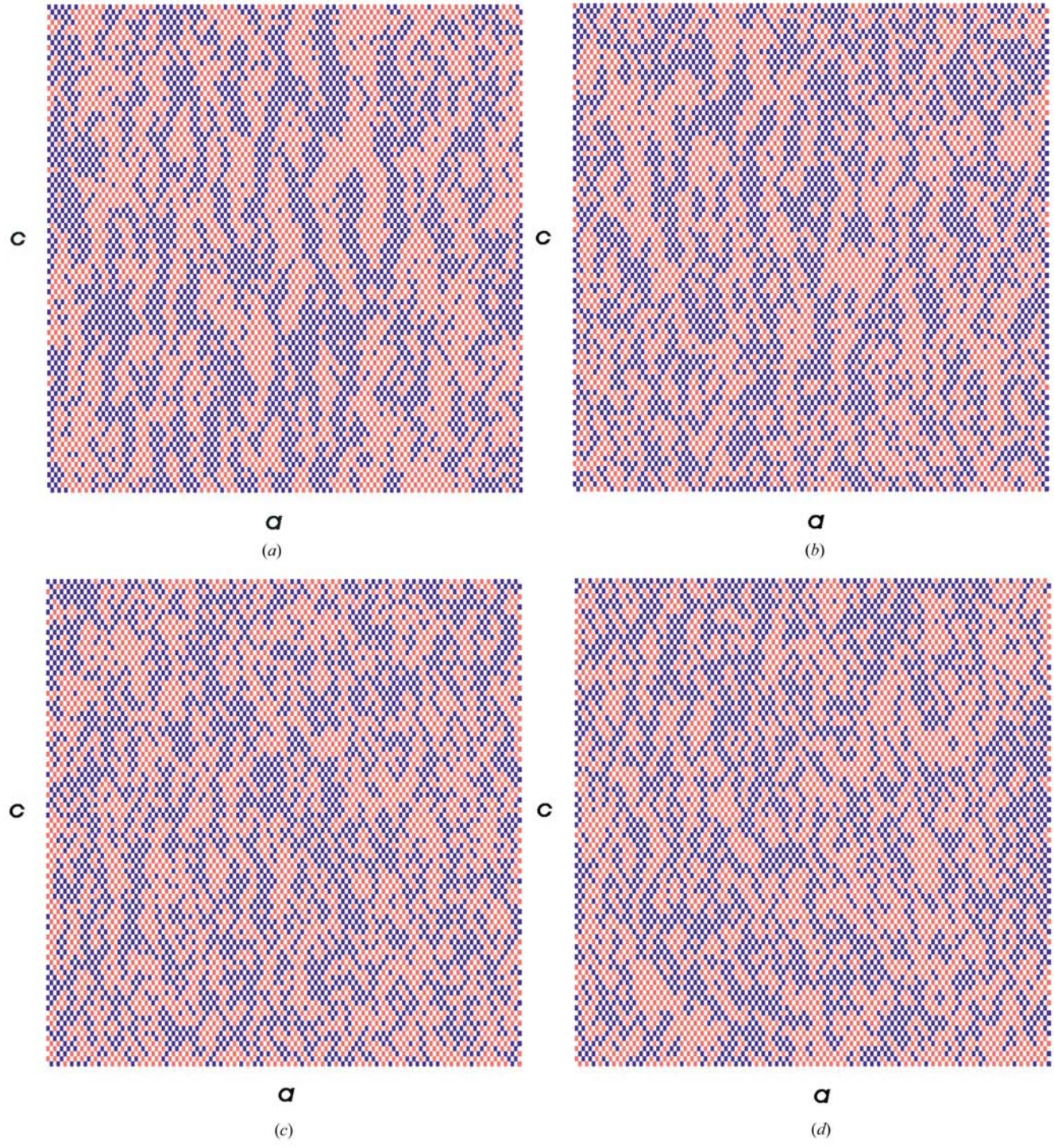

Figure 5
Distribution of (+)- and (−)-$[Na^+NO_2^-]_\infty$ rows passing through 0,0,0 and $\frac{1}{2}$,0,$\frac{1}{2}$ sites in the (010) plane of 70 × 48 lattice cells with the short- and medium-range order revealed by RMC: (*a*) at 438 K, (*b*) at 442 K, (*c*) at 460 K and (*d*) at 480 K. Orange rectangles: (+) rows; blue rectangles: (−) rows.

438 K obtained by the RMC simulation of only a small section of the diffraction pattern. Satisfactory agreement of reconstructed and calculated layers confirms our assumptions and validates the results obtained.

5. Temperature dependence of the medium- and short-range order in the paraelectric short-range modulated phase of $NaNO_2$

Distributions of (+)- and (−)-$[Na^+NO_2^-]_\infty$ rows passing through 0,0,0 and $\frac{1}{2},0,\frac{1}{2}$ sites in the (010) plane at consecutive temperatures of 438, 442, 460 and 480 K as revealed by RMC simulation are presented in Figs. 5(*a*)–(*d*). Orange rectangular spots mark (+)-$[Na^+NO_2^-]_\infty$ rows and blue ones mark (−)-$[Na^+NO_2^-]_\infty$ rows of opposite polarity. The distributions of (+) and (−) rows at 438 and 442 K reveal characteristic nanodomains which are remnants of the highly distorted modulated structure of the antiferroelectric phase. With increasing temperature the distortion of the sinusoidal modulation proceeds, and at 460 and 480 K nanodomains become difficult to see. Diffraction patterns also differ considerably. At 460 and 480 K diffuse satellite reflections are replaced by broad diffuse streaks.

Pair correlation coefficients $c[u00]$ and $c[00w]$ (Neder & Proffen, 1997) between pairs of sites in the (010) plane crossed by (+)- or (−)-$[Na^+NO_2^-]_\infty$ chains and separated by $[u00]$ or $[00w]$ were calculated using the procedure described in our earlier papers (Krawczyk *et al.*, 2002, 2003). Correlations $c[00w]$ decay continuously with increasing distance. At 438 K $c[00w]$ becomes zero when $w \simeq 8$, which is a measure of the average length of nanodomains in the [001] direction. The length of nanodomains decreases with increasing temperature. Correlations $c[u00]$ have a minimum at *ca* $u = 3$ and a weak broad maximum at *ca* $u = 8$ connected with remnants of the sinusoidal modulation of the antiferroelectric phase. The average modulation length of *ca* 8 also follows from the distance between the maxima of $(0-\sigma)42$ and $(0+\sigma)42$ diffuse satellite reflections.

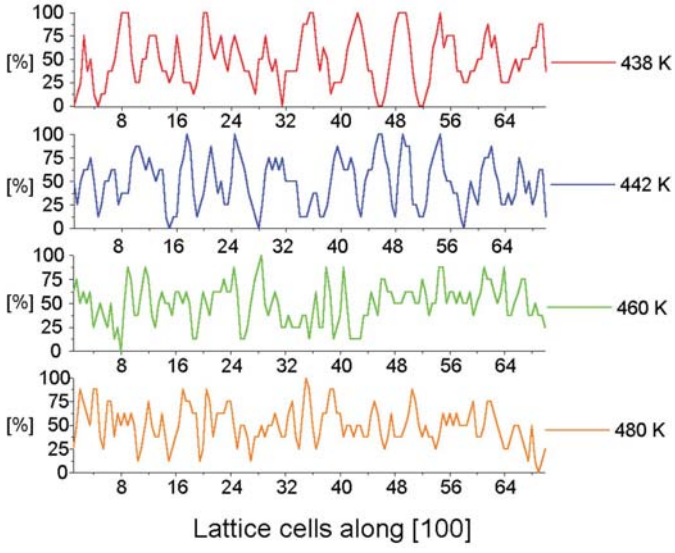

Figure 6
Remnants of the distorted sinusoidal modulation. Percentage of (+)-$[Na^+NO_2^-]_\infty$ chains passing through 0,0,0 and $\frac{1}{2},0,\frac{1}{2}$ sites in a strip of $70a \times 10c$ lattice cells in the (010) plane at 438, 442, 460 and 480 K along the [100] direction.

The remnants of the sinusoidal modulation are also presented in Fig. 6, which shows the percentage of (+)-$[Na^+NO_2^-]_\infty$ chains passing through 0,0,0 and $\frac{1}{2},0,\frac{1}{2}$ sites in a strip of 70×10 lattice cells in the (010) plane of $NaNO_2$ in the short-range modulated paraelectric phase at temperatures of 438, 442, 460 and 480 K along the [100] direction.

6. Conclusions and summary

In our previous papers (Krawczyk *et al.*, 2002, 2003) we investigated the definition of the diffuse superstructure reflections of a disordered crystal structure with short- or medium-range order. The present paper is devoted to the study of diffuse satellite reflections, focusing on the short- and medium-range modulated crystal structure with remnants of distorted fragments of a sinusoidal modulation. This is a new type of disordered crystal structure with remnants of a sinusoidal modulation.

The crystal structure of paraelectric sodium nitrite can be regarded as consisting of (+)- and (−)-$[Na^+NO_2^-]_\infty$ polar rows perpendicular to the (010) plane. The infinite rows were assumed to be of uniform polarity. Distributions at consecutive temperatures 438, 442, 460 and 480 K of (+)- and (−)-$[Na^+NO_2^-]_\infty$ rows crossing the (010) plane revealed by RMC simulation show nanodomains elongated in the [001] direction which are remnants of distorted fragments of the sinusoidally modulated crystal structure of antiferroelectric $NaNO_2$.

The size of the nanodomains and the range of order in the paraelectric $NaNO_2$ crystal structure decreases with temperature. With increasing temperature the sinusoidal modulation distortion proceeds and at 460 and 480 K the nanodomains become very small. Diffraction patterns also differ considerably. At 460 and 480 K diffuse satellite reflections are replaced by broad diffuse streaks.

All data were collected after heating the crystal specimen up to selected temperatures. In a separate experiment the specimen was kept for 30 min at 500 K. The diffraction pattern recorded after cooling the crystal slowly down to 438 K was almost the same as that recorded after heating the sample to the same temperature. This indicates that the crystal structure of the short-range modulated phase of $NaNO_2$ does not depend on thermal history.

The study of the temperature dependence of short-range order in ferroelectric $NaNO_2$ on approaching the Curie point is in progress.

We are obliged to Dr Jolanta Krawczyk for useful comments and discussions.

References

Boehm, H. (1978). *Z. Kristallogr.* **148**, 207–220.
Canut, M. & Hosemann, R. (1964). *Acta Cryst.* **17**, 973–981.

Gohda, T., Ichikawa, M., Gustafsson, T. & Olovsson, I. (2000). *Acta Cryst.* B**56**, 11–16.
Hoshino, S. & Motegi, H. (1967). *Jpn. J. Appl. Phys.* **6**, 708–718.
Ichikawa, M., Gustafsson, T. & Olovsson, I. (2002). *Solid State Commun.* **123**, 135–139.
Kay, M. I., Frazer, B. C. & Ueda, R. (1992). *Phase Transit.* **38**, 127–220.
Kay, M. I., Gonzabo, J. A. & Maglic, R. (1975). *Ferroelectrics*, **9**, 179–186.
Komatsu, K., Itoh, K. & Nakamura, E. (1988). *J. Phys. Soc. Jpn*, **57**, 2836–2840.
Krawczyk, J. (2002). Personal communication.
Krawczyk, J., Pietraszko, A., Kubiak, R. & Łukaszewicz, K. (2003). *Acta Cryst.* B**59**, 384–392.
Krawczyk, J., Pietraszko, A. & Łukaszewicz, K. (2002). *Acta Cryst.* B**58**, 622–826.
Kucharczyk, D., Pietraszko, A. & Łukaszewicz, K. (1976). *Phys. Status Solidus*, **37**, 287–294.
Kucharczyk, D., Pietraszko, A. & Łukaszewicz, K. (1978). *Ferroelectrics*, **21**, 445–447.
Neder, R. & Proffen, Th. (1997). *J. Appl. Cryst.* **30**, 171–175
Sawada, S., Nomura, S., Fujii, S. & Yoshida, I. (1958). *Phys. Rev. Lett.* **1**, 320.
Tanisaki, S. (1961). *J. Phys. Soc. Jpn*, **16**, 579.
Yamada, Y., Shibuya, I. & Hoshino, S. (1963). *J. Phys. Soc. Jpn*, **18**, 1594–1603.
Ziegler, G. E. (1931). *Phys. Rev.* **38**, 1040–1047.